Appl. Phys. A (2015) 119:1609–1613
DOI 10.1007/s00339-015-9144-x

Applied Physics A
Materials Science & Processing

CrossMark

# Hopping conduction properties of the Sn:SiO$_X$ thin-film resistance random access memory devices induced by rapid temperature annealing procedure

**Kai-Huang Chen[1] · Kuan-Chang Chang[2] · Ting-Chang Chang[3,4] · Tsung-Ming Tsai[2] · Kuo-Hsiao Liao[2] · Yong-En Syu[5] · Simon M. Sze[6]**

Received: 23 February 2015 / Accepted: 30 March 2015 / Published online: 17 April 2015
© Springer-Verlag Berlin Heidelberg 2015

**Abstract** Bipolar switching properties and electrical conduction mechanism in Sn:SiO$_X$ thin-film RRAM devices were investigated and discussed. To complete the resistive switching properties of the stannum doped into silicon oxide thin films, the RTA-treated Sn:SiO$_X$ thin-film RRAM devices were investigated and discussed. In addition, the improvement qualities and electrical switching properties of the RTA-treated Sn:SiO$_X$ thin-film RRAM devices were carried out XPS, FT-IR, and IV measurement. The ohmic conduction with metal-like behavior and hopping conduction dependent activation energy properties by the Arrhenius plot equation in LRS of the Sn:SiO$_X$ thin films was investigated. The activation energy and hopping distance for the RTA-treated thin films were found to be 0.018 eV and 1.1 nm, respectively. For the compatibility with the IC processes, the RTA treatment was a promising method for the Sn:SiO$_X$ thin-film RRAM nonvolatile memory applications.

✉ Kai-Huang Chen
d9131802@gmail.com

1 Department of Electronics Engineering and Computer Science, Tung-Fang Design Institute, Kaohsiung, Taiwan

2 Department of Materials and Optoelectronic Science, National Sun Yat-sen University, Kaohsiung, Taiwan

3 Department of Physics, National Sun Yat-sen University, Kaohsiung, Taiwan

4 Advanced Optoelectronics Technology Center, National Cheng Kung University, Tainan, Taiwan

5 Department of Mechanical and Electro-Mechanical Engineering, National Sun Yat-sen University, Kaohsiung, Taiwan

6 Department of Electronics Engineering, National Chiao Tung University, Hsinchu, Taiwan

## 1 Introduction

Many volatile and nonvolatile memory devices are used for application in various portable electronic devices such as, static random access memory (SRAM), dynamic random access memory (DRAM), ferroelectric random access memory (FeRAM), magnetron random access memory (MRAM), and phrase change random access memory (PRAM). However, the resistive random access memory (RRAM) devices will be widely investigated and discussed in the future. To excellent memory characteristics, high storage capacity, long retention cycles, low operation voltage, and low electric consumption, the RRAM devices are continuously selected and discussed for applications in the sunrise nonvolatile memory devices [1–8].

Silicon-based oxide materials for co-sputtering technology are widely investigated and developed for applications in high storage capacity of nonvolatile RRAM devices. The silicon-based oxide RRAM devices are widely investigated because of its compatibility integrated circuit (IC) processes, long retention cycles, low operation voltage, and low electric consumption [9–15].

The rapid thermal annealing (RTA) processing is indispensable and essential technology for crystallization and quality of the dielectric thin films. Besides, the budget cost and fabrication time of the RTA are much lower than others [4]. In this study, the electrical properties of the Sn:SiO$_X$ thin-film RRAM devices were improved by the RTA procedure. To explain the resistive switching mechanism for the RTA procedure on the stannum-doped $SiO_2$ layer dominated by interface of TiN electrode or Sn:SiO$_X$ film, the Pt/ Sn:SiO$_X$ TiN device was fabricated in virtue of inertia of Pt electrode as top electrode. Besides, the electrical switching properties and hopping conduction of the low

resistance state (LRS) and the high resistance state (HRS) of the Sn:$SiO_X$ thin-film RRAM devices were also used and discussed later.

## 2 Experimental details

Metal-insulator-metal (MIM) device, schematically shown in Fig. 1a, was fabricated over a polished p-Si wafer of nominal resistively ~1.0 Ω cm. To overcome the existence of native oxide on p-type silicon wafer, the particle and metal ion on p-type silicon wafer were removed during RCA clean process. As shown in Fig. 1a, the MIM structure samples were divided to discuss the feasibility of RRAM properties by $SiO_2$ and stannum co-sputtering technology with pure $SiO_2$ and stannum targets. The metal and silicon dioxide target was placed near 5–8 cm away from the substrate. In order to remove the defects of metal target and obtain stable plasma during deposition time, pre-sputtering time of as-deposited oxide thin film was maintained for 30 min under argon ambient. The sputtering power was the rf power of 200 W and dc power of 10 W for silicon dioxide and stannum targets, respectively. For RTA process, the Sn:$SiO_X$ thin-film RRAM devices were annealed and treated at 200 °C for 30 s. In addition, the Pt top electrode with a thickness of 200 nm was deposited on Sn:$SiO_X$ film to form Pt/ Sn:$SiO_X$ / TiN MIM structure by dc sputtering. The typical *I*–*V* characteristics of Sn:$SiO_X$ RRAM devices are obtained by Agilent B1500 semiconductor parameter analyzer. Besides, X-ray photoelectron spectroscopy (XPS) and Fourier-transform infrared spectrometer (FT-IR) are used to analyze the chemical composition and bonding of the non-treated and RTA-treated Sn:$SiO_X$ thin films, respectively.

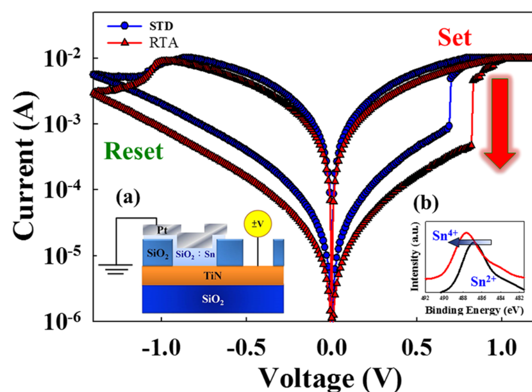


**Fig. 1** The typical bipolar behavior of the Sn:$SiO_X$ thin-film RRAM devices for RTA process, *a* using the metal-insulator-metal (MIM) structure, *b* binding energy for $Sn^{2+}$ and $Sn^{4+}$

## 3 Results and discussion

The structure of Sn:$SiO_X$ RRAM devices are shown in Fig. 1a. After the forming process at a voltage of 20 V, the Sn:$SiO_X$ thin-film RRAM devices were reached a high resistance state (HRS) and low resistance state (LRS). The compliance current was 10 mA. By sweeping the bias to negative over the reset voltage, a gradual decrease in current was presented to switch the cells from LRS to HRS (reset process). Conversely, the device cell turns back to LRS while applying a high positive bias than the set voltage (set process). In order to further investigate the resistance switching behaviors in non-treated and RTA-treated Sn:$SiO_X$ thin-film RRAM devices, the conduction mechanisms of HRS and LRS in *I*–*V* curves were fitting and discussed.

Figure 1 shows the bipolar behavior of the non-treated and RTA-treated Sn:$SiO_X$ thin-film RRAM devices by applying base on Pt and TiN electrode. As shown in Fig. 1, the LRS and HRS of the RTA-treated Sn:$SiO_X$ thin-film RRAM devices exhibited the low dropping progressively. The RTA-treated Sn:$SiO_X$ thin film was exhibited the low current density for the defects and dangling bonds decreased. To discuss and investigate the influence of the stannum element of RTA-treated thin film, the chemical composition characteristics were found and analyzed by the XPS and FI-IR measurement. In Fig. 1b, the binding energy of the non-treated and RTA-treated thin films was 486.8 and 487.6 eV. For the RTA-treated Sn:$SiO_X$ thin films, it was caused by the $Sn^{2+}$ binding oxidation and repaired to form $Sn^{4+}$ binding. The Si–O–Si symmetric and Sn–O bonds of non-treated thin films were 800 and 650 $cm^{-1}$ from FT-IR measurement. In Fig. 2, the peak intensity and the amount of Sn–O bonds in Sn:$SiO_X$ thin

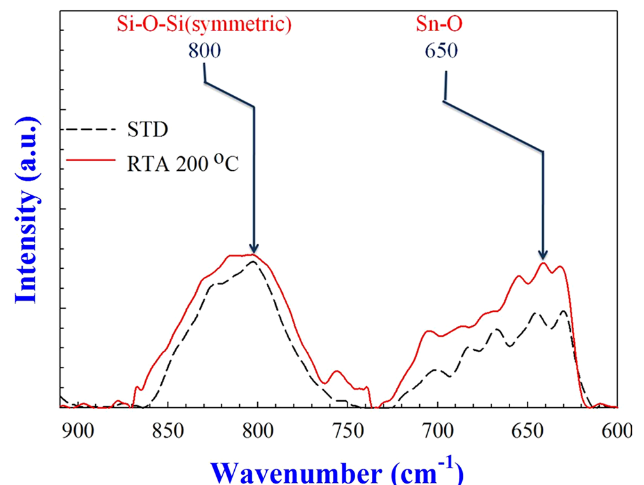


**Fig. 2** The Si–O–Si symmetric and Sn–O bond of non-treated and RTA-treated Sn:$SiO_X$ thin-film RRAM devices

films were increased and it was caused by re-oxidation in RTA process.

To discuss the resistance switching mechanisms, the HRS of the non-treated and RTA-treated Sn:SiO$_X$ thin-film RRAM devices were investigated and fitting in Fig. 3a. As shown in Fig. 3b, c, the non-treated and RTA-treated Sn:SiO$_X$ thin film exhibited the Poole–Frenkel conduction and Schottky conduction by ln($I/V$)–$V^{1/2}$ and ln($I$)–$V^{1/2}$ curves. For non-treated thin film, the doping stannum into SiO$_2$ of the Sn:SiO$_X$ thin films resulted in an increased amount of hetero-defects. Additionally, the electrons were transferred through the hetero-defects to make the current conduction mechanism dominated by Poole–Frenkel conduction mechanism. Besides, the RTA-treated Sn:SiO$_X$ thin film exhibited low current density and Schottky emission mechanism, it caused and happened by the defects and dangling bonds decreased [16–18].

In Fig. 4b, c, the non-treated and RTA-treated Sn:SiO$_X$ thin film exhibited the ohmic conduction and hopping conduction by ln($I$)–ln($V$) and ln($I$)–$V$ curves. In set process region, the transmission current was directly flowed and formed by the intrinsic carrier in Sn:SiO$_X$ thin film, and it was increased by the applied voltage increased. The stannum atom clustered in metallic filament of the Sn:SiO$_X$ thin film, showing the ohmic conduction in LRS state [16–18]. The hopping conduction mechanism was caused by shallow trapped electrons surpass to the activation energy barrier and form the leakage current in discontinuous and broken metallic filament of the Sn:SiO$_X$ thin film. In order to investigate the activation energy from the hopping conduction mechanism, the $-\ln(I)$ versus $(1/kT)$ curves of the Arrhenius plot equation for non-treated and RTA-treated Sn:SiO$_X$ thin-film RRAM devices were used. According to the relationship of hopping conduction, $E_{a,\exp} = -\partial \log I/\partial(1/kT)$ where $E_a$ is active energy, $k$ is the Boltzmann's constant, and $T$ is the absolute temperature [17].

To discuss the hopping conduction and activation energy relationship properties, the LRS of the Sn:SiO$_X$ thin-film RRAM devices for the voltage of 0.3 V was calculated by the Arrhenius plot equation. The activation energy equation is $E_{a,\exp} = -\frac{\partial \log I}{\partial\left(\frac{1}{kT}\right)}$ where $E_a$ is active energy, $k$ is the Boltzmann's constant, and $T$ is the absolute temperature. According to the $-\ln(I)$ versus $(1/kT)$ curves of the Arrhenius plot equation in Fig. 5, the activation energy extraction for the non-treated and RTA-treated was found to be 0.0225 and 0.018 eV (inset of Fig. 5), respectively. The RTA process induced the activation energy barrier lowering of the Sn:SiO$_X$ thin film due to its stannum atom being continuously clustered.

Additionally, the hopping conduction distance will be an important factor to activation energy barrier of the experimental result. The hopping conduction distance of the RTA-treated and non-treated Sn:SiO$_X$ thin film was also calculated and discussed by the hopping distance extraction equation. The hopping distance extraction equation is: $E_{a,\exp} = -\frac{\partial \log I}{\partial\left(\frac{1}{kT}\right)} = E_C - E_F - qV_A\frac{\Delta z}{2u_a}$ where $E_a$ is active energy, $k$ is the applied voltage, $\Delta z$ is the average inter-trap distance, and $u_a$ is about the thickness of 30 nm. In Fig. 6, the hopping conduction distance of the Sn:SiO$_X$ RRAM devices for the RTA-treated process was about 1.1 nm.

To investigated the reliability and endurance properties in the Sn:SiO$_X$ thin-film RRAM devices, the different

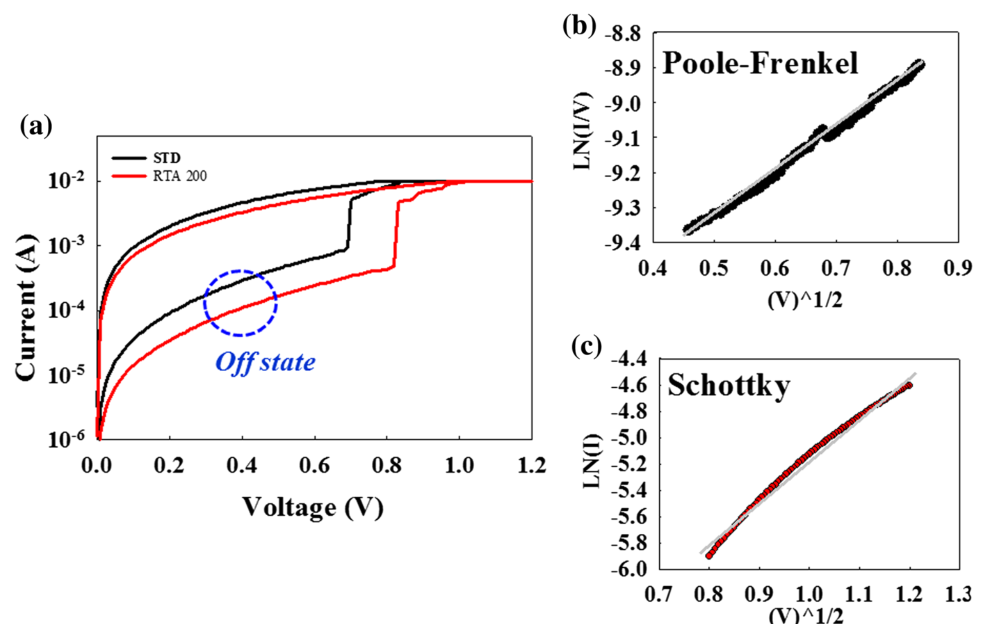


**Fig. 3** Electrical characteristics of the high resistance state (HRS) in the Sn:SiO$_X$ thin-film RRAM devices for RTA process with **a** $I$–$V$ curves, **b** ln($I$) versus $V^{1/2}$ curves, and **c** ln($I/T^2$) versus $V^{1/2}$ curves

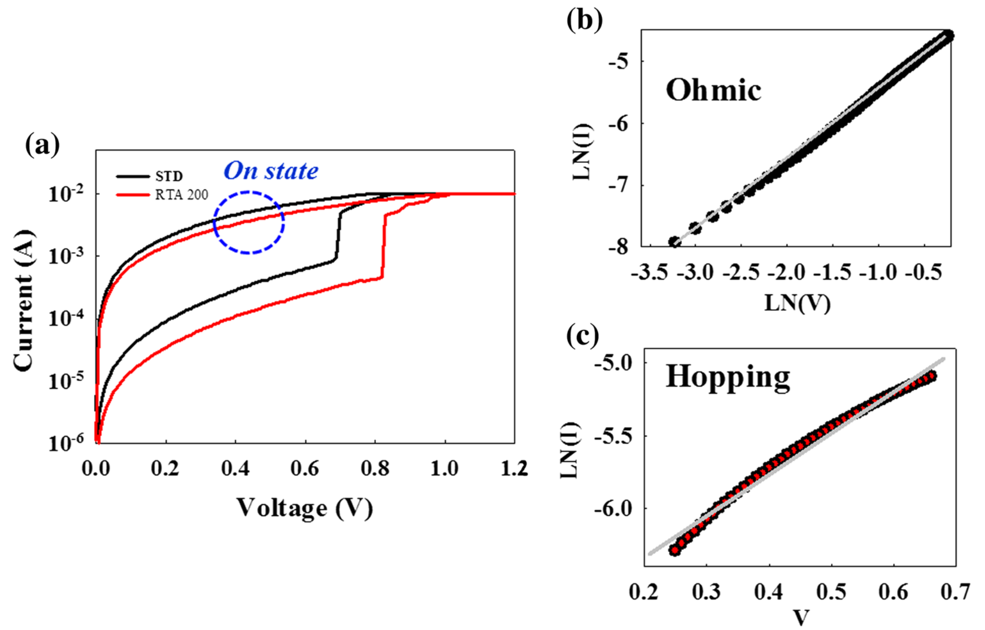


**Fig. 4** Electrical characteristics of the low resistance state (LRS) in the Sn:$SiO_X$ thin-film RRAM devices for RTA process with **a** *I–V* curves, **b** ln(*I*) versus ln(*V*) curves, and **c** ln(*I*) versus *V* curves

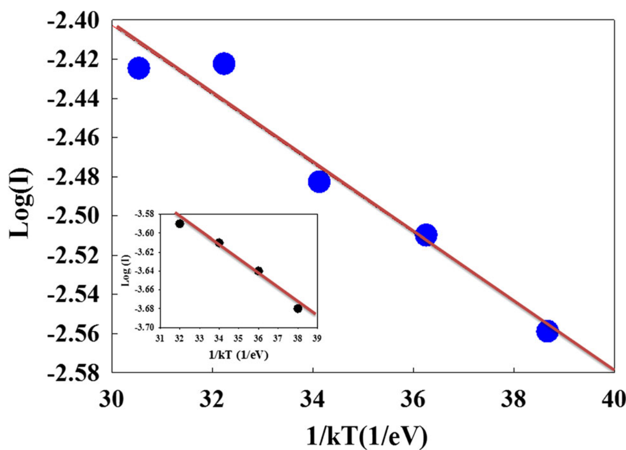


**Fig. 5** The activation energy of the non-treated and RTA-treated Sn:$SiO_X$ thin-film RRAM devices with a plot of ln(*I*) versus (1/*kT*) curves

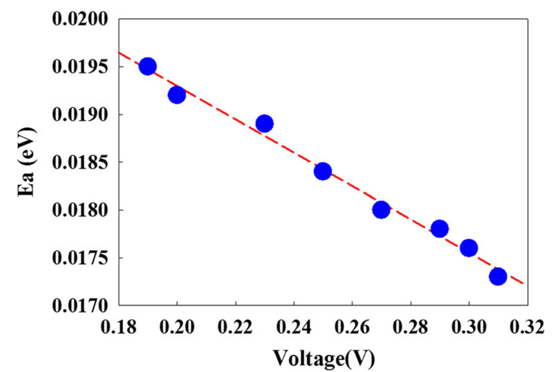


**Fig. 6** The hopping conduction distance of non-treated and RTA-treated Sn:$SiO_X$ thin-film RRAM devices with a plot of ($E_a$) versus *V* curves

switching cycle and times were measured and obtained. The switching cycling was measured another type of the retention characteristics in Fig. 7. The stable switching property in the HRS and LRS was about for $10^6$ cycles. As shown in Fig. 8, no significant change in the current values for $10^4$ s and 85 °C was observed. In addition, the low-/high-resistance ratio value was maintained about 1 order. In addition, the result shows remarkable endurance properties of the Sn:$SiO_X$ thin-film RRAM for applications in nonvolatile memory devices.

To prove the hopping conduction in LRS, the atoms structure of the RTA-treated Sn:$SiO_X$ thin-film RRAM devices was described and explained in Fig. 9. The oxygen atoms of dangling bond in $SiO_2$ were formed in thin films and

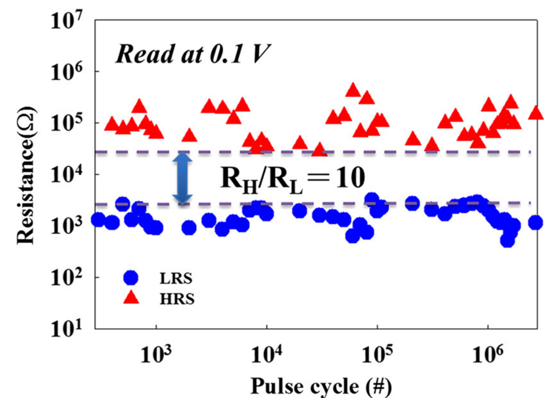


**Fig. 7** Switching cycling of the RTA-treated Sn:$SiO_X$ thin-film RRAM devices measured at 0.5 V

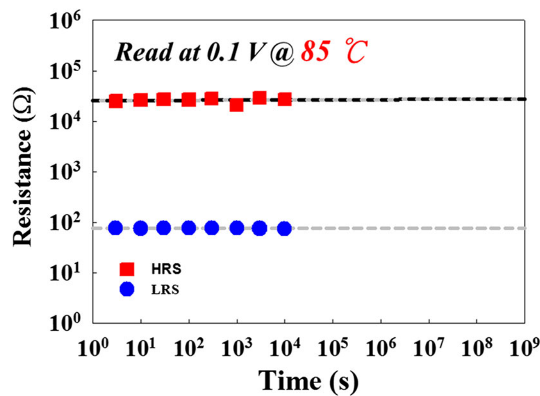


**Fig. 8** Retention characteristics of the RTA-treated Sn:SiO$_X$ thin-film RRAM devices measured at 0.5 V

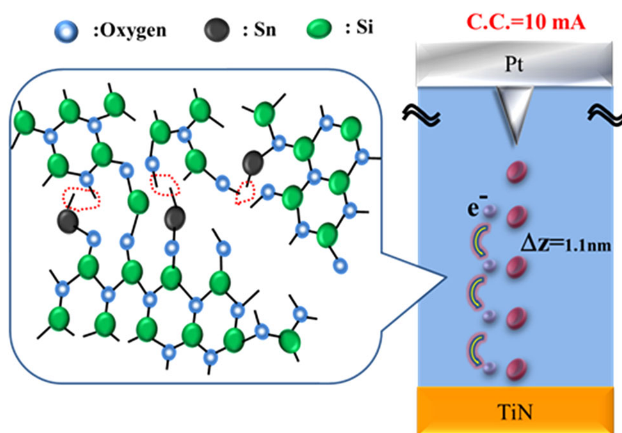


**Fig. 9** The atoms structure and hopping conduction mechanism of the RTA-treated Sn:SiO$_X$ thin-film RRAM devices for compliance current of 10 mA

exhibited the ohmic conduction mechanism. However, the ohmic conduction transferred to hopping conduction mechanism of Sn:SiO$_X$ thin films was caused by $Sn^{2+}$ binding oxidation and repaired to form $Sn^{4+}$ binding after the RTA process. The oxygen atoms and stannum element of Sn:SiO$_X$ thin film were re-oxidation and repaired. The hopping conduction distance of the RTA-treated Sn:SiO$_X$ RRAM devices was formed and found to be 1.1 nm in Fig. 9.

## 4 Conclusion

In conclusion, the bipolar switching properties of the thin-film RRAM devices were formed and enhanced by the rapid temperature annealing process because of the low melting point of the stannum element and oxidation in the crystal lattice. For XPS results obtained, it was found by the $Sn^{2+}$ binding of the RTA-treated Sn:SiO$_X$ thin-film oxidation and repaired to form $Sn^{4+}$ binding. For the LRS, the non-treated and treated thin films were exhibited the ohmic conduction with metal-like behavior and hopping conduction, respectively. For the HRS, the non-treated and treated thin films were exhibited the Poole–Frenkel conduction and Schottky emission conduction, respectively. To the Arrhenius plot equation, the activation energy extraction of the Sn:SiO$_X$ RRAM devices for the non-treated and RTA-treated was found to be 0.0225 and 0.018 eV, respectively. For the thickness of 30 nm, the hopping conduction distance for the RTA-treated was calculated to 1.1 nm. To the activation energy barrier lowering and the short hopping conduction distance of electrical conduction path, the rapid temperature annealing process effect induced the metal atom continuously clustered and the electronic easily jump the low potential well of the Sn:SiO$_X$ thin-film RRAM devices in this study.

**Acknowledgments** The authors acknowledge the financial support from the National Science Council of the Republic of China (NSC 102-2633-E-272-001).

## References

1. C.T. Tsai, T.C. Chang, P.T. Liu, P.Y. Yang, Y.C. Kuo, K.T. Kin, P.L. Chang, F.S. Huang, Appl. Phys. Lett. **91**(1), 012109 (2007)
2. C.T. Tsai, T.C. Chang, K.T. Kin, P.T. Liu, P.Y. Yang, C.F. Weng, F.S. Huang, J. Appl. Phys. **103**(7), 074108 (2008)
3. M.C. Chen, T.C. Chang, S.Y. Huang, K.C. Chang, H.W. Li, S.C. Chen, J. Lu, Y. Shi, Appl. Phys. Lett. **94**, 162111 (2009)
4. K.H. Chen, T.C. Chang, G.C. Chang, Y.E. Hsu, Y.C. Chen, H.Q. Xu, Appl. Phys. A: Mater. Sci. Process. **99**(1), 291–295 (2010)
5. P.C. Yang, T.C. Chang, S.C. Chen, Y.S. Lin, H.C. Huang, D.S. Gan, Electrochem. Solid State Lett. **14**(2), H93–H95 (2011)
6. Y.E. Syu, T.C. Chang, T.M. Tsai, Y.C. Hung, K.C. Chang, M.J. Tsai, M.J. Kao, S.M. Sze, IEEE Electron Device Lett. **32**(4), 545–547 (2011)
7. L.W. Feng, C.Y. Chang, Y.F. Chang, W.R. Chen, S.Y. Wang, P.W. Chiang, T.C. Chang, Appl. Phys. Lett. **96**, 052111 (2010)
8. L.W. Feng, C.Y. Chang, Y.F. Chang, T.C. Chang, S.Y. Wang, S.C. Chen, C.C. Lin, S.C. Chen, P.W. Chiang, Appl. Phys. Lett. **96**, 222108 (2010)
9. K.H. Chen, Y.C. Chen, C.F. Yang, T.C. Chang, J. Phys. Chem. Solids **69**, 461 (2008)
10. C.F. Yang, K.H. Chen, Y.C. Chen, T.C. Chang, I.E.E.E. Trans, Ultrason. Ferroelectr. Freq. Control **54**, 1726 (2007)
11. C.F. Yang, K.H. Chen, Y.C. Chen, T.C. Chang, Appl. Phys. A **90**, 329 (2008)
12. K.H. Chen, Y.C. Chen, Z.S. Chen, C.F. Yang, T.C. Chang, Appl. Phys. A **89**, 533 (2007)
13. K.H. Chen, C.H. Chang, C.M. Cheng, C.F. Yang, Appl. Phys. A **97**, 919 (2009)
14. K.H. Chen, C.M. Cheng, C.C. Shih, J.H. Tsai, Appl. Phys. A **103**, 1173 (2011)
15. C.M. Cheng, K.H. Chen, J.H. Tsai, C.L. Wu, Ceram. Int. **38**, S87 (2012)
16. C. Alessandro, F. Massimo, I. Daniele, F. Paolo, IEEE Electron Device Lett. **31**(9), 1023–1025 (2010)
17. T.Y. Tseng, H. Nalwa, *Hand book of nanoceramics and their based nano devices* (American Scientific Publishers, USA, 2009), pp. 175–176
18. Daniele Ielmini, J. Appl. Phys. **102**(5), 054517 (2007)